

Enhanced Steatosis and Fibrosis in Liver of Adult Offspring Exposed to Maternal High-Fat Diet

Michael D. Thompson,* Mary J. Cismowski,† Aaron J. Trask,‡ Scott W. Lallier,‡ Amanda E. Graf,‡ Lynette K. Rogers,‡ Pamela A. Lucchesi,†§ and David R. Brigstock¶

*Division of Endocrinology, Nationwide Children’s Hospital, Columbus, OH, USA

†Center for Cardiovascular and Pulmonary Research, Nationwide Children’s Hospital, Columbus, OH, USA

‡Center for Perinatal Research, Nationwide Children’s Hospital, Columbus, OH, USA

§Department of Basic Sciences, The Commonwealth Medical College, Scranton, PA, USA

¶Center for Clinical and Translational Research, Nationwide Children’s Hospital, Columbus, OH, USA

Early life exposures can increase the risk of developing chronic diseases including nonalcoholic fatty liver disease. Maternal high-fat diet increases susceptibility to development of steatosis in the offspring. We determined the effect of maternal high-fat diet exposure in utero and during lactation on offspring liver histopathology, particularly fibrosis. Female C57Bl/6J mice were fed a control or high-fat diet (HFD) for 8 weeks and bred with lean males. Nursing dams were continued on the same diet with offspring sacrificed during the perinatal period or maintained on either control or high-fat diet for 12 weeks. Increased hepatocyte proliferation and stellate cell activation were observed in the liver of HFD-exposed pups. Offspring exposed to perinatal high-fat diet and high-fat diet postweaning showed extensive hepatosteatorosis compared to offspring on high-fat diet after perinatal control diet. Offspring exposed to perinatal high-fat diet and then placed on control diet for 12 weeks developed steatosis and pericellular fibrosis. Importantly, we found that exposure to perinatal high-fat diet unexpectedly promotes more rapid disease progression of nonalcoholic fatty liver disease, with a sustained fibrotic phenotype, only in adult offspring fed a postweaning control diet.

Key words: Developmental origins of disease; Fatty liver; High-fat diet (HFD); Fibrosis; Stellate cell activation

INTRODUCTION

As childhood obesity rates continue to climb, metabolic syndrome and its complications have become more prevalent in the pediatric population. Along with being the primary liver manifestation of metabolic syndrome, nonalcoholic fatty liver disease (NAFLD) is quickly becoming the most common chronic liver disease in children. The estimated prevalence of NAFLD in children is 3–10%, and, more strikingly, 70–90% of obese children have NAFLD^{1,2}. NAFLD covers a broad spectrum of disease that is characterized by simple steatosis at the lower end of the spectrum and nonalcoholic steatohepatitis (NASH) at the higher end. The histologic features of NASH include inflammation, hepatocyte ballooning, cell death, and fibrosis. More progressive disease leaves the patient at increased risk for liver failure and/or hepatocellular carcinoma. The pathogenesis and disease progression

of NAFLD are of significant research interest, as there is currently no effective pharmacologic therapy.

While an emphasis has been placed on understanding the metabolic factors that lead to the initial development of NAFLD, it is still not clear why some patients are more prone to disease progression from NASH to fibrosis. One area of growing interest is the idea that in utero and early life exposures may have a sustained impact on susceptibility to chronic diseases later in life, known as the developmental origins of health and disease (DOHaD)^{3,4}. Important epidemiologic and experimental studies indicate that a poor nutritional environment in utero increases the risk of developing conditions such as type 2 diabetes, cardiovascular disease, and NAFLD⁵. As 60% of women in the US are overweight at time of conception, it has become increasingly important to understand the consequences of maternal obesity on the health of offspring⁶. While there is a clear association

Address correspondence to Michael D. Thompson, M.D., Ph.D., Division of Endocrinology, Nationwide Children’s Hospital, 700 Children’s Drive, Columbus, OH 43205, USA. Tel: (614) 722-3153; Fax: (614) 722-4440; E-mail: michael.thompson@nationwidechildrens.org

between maternal prepregnancy weight and the development of early childhood obesity^{7,8}, it is possible that this association extends to the development of NAFLD in children.

Studies utilizing animal models of maternal high-fat diet (HFD) exposure have shown a clear predisposition to develop fatty liver disease in offspring. Exposure to a HFD in utero and during lactation increases the propensity for development of NAFLD in both mice and rats^{9–11}. Similar findings were observed in a nonhuman primate model¹². These studies demonstrated earlier development of hepatic steatosis as well as more rapid progression to NASH was observed when the animals resumed a HFD in adulthood. Interestingly, mice exposed to a HFD in utero and during lactation developed hepatic steatosis despite being placed on a control diet (CD) postweaning¹⁰. This indicates that changes occur while in utero and/or during lactation that persist into adulthood. Indeed, it has been proposed that this early life insult may be the “first hit” in the “two-hit hypothesis” in relation to the development of NAFLD and NASH¹³.

While it is clear that in utero exposure to HFD predisposes to development of NAFLD and likely NASH, no study to date has evaluated whether such exposure increases the susceptibility to development of liver fibrosis or affects hepatic stellate cells (HSCs), the primary cell involved in matrix production in the liver. Understanding this role is of critical importance as fibrosis is the primary predictor of outcomes in patients with NAFLD in relation to liver-related complications, need for transplantation, and mortality¹⁴. In the current study, we sought to evaluate perinatal liver pathology in the setting of exposure to maternal HFD, as well as the risk for disease progression to fibrosis in adulthood. We hypothesized that maternal HFD exposure would induce stellate cell activation in the perinatal period and predispose the offspring to progression to liver fibrosis with continued exposure to a HFD.

MATERIALS AND METHODS

Animal Model

All animal studies were approved by the Institutional Animal Use and Care Committee at Nationwide Children’s

Hospital. Three-week-old female C57Bl/6J mice were purchased from The Jackson Laboratories. Mice were housed under a 12-h light/dark cycle at 22°C and 60% humidity. They were allowed ad libitum access to water and food. After 1 week of acclimatization, mice were randomly assigned to either a HFD (60.3% kcal fat, 21.3% kcal carbohydrate, 18.4% kcal protein; TD.06414; Harlan Teklad, Indianapolis, IN, USA) or a CD (10.4% kcal fat, 69.1% kcal carbohydrate, 20.5% kcal protein; TD.08806; Harlan Teklad) and were weighed weekly. Food was stored at 4°C and replaced in cages weekly to prevent degradation. At the start of the ninth week on experimental diet, the female mice were continuously paired for breeding with control male mice for 2 weeks. A subset of females was sacrificed for tissue collection at the start of the ninth week prior to pairing. Male mice were maintained on standard chow except for the 2-week breeding periods when they were exposed to the respective experimental diet. Pregnant mice were individually housed prior to giving birth. Offspring were kept with the same dam during lactation. For perinatal analysis, offspring were sacrificed at 0, 7, 14, and 21 days of life ($n \geq 4$ per group). For long-term feeding studies, offspring at time of weaning (at 3 weeks of age) were assigned to either HFD or CD and maintained on that diet for 12 weeks ($n = 4–9$ of each gender within each group) (Fig. 1). Body weight was monitored weekly, and fasting (≥ 8 h) glucose levels were measured at 4-week intervals. Food intake was estimated each week by calculating the amount of food consumed in each cage and dividing by the number of mice in the cage. At time of sacrifice, body weight was recorded, and the liver was weighed and dissected. The dissected liver was divided and either placed in 10% neutral buffered formalin or snap frozen in liquid nitrogen and stored at -80°C until analyzed. Data shown are from male offspring except when sex is noted.

Histology, Immunohistochemistry, and Special Stains

Tissues fixed in 10% formalin were embedded in paraffin, and 5- μm sections were cut and used for hematoxylin and eosin (H&E) staining, Sirius red staining, terminal deoxynucleotidyl transferase dUTP nick end

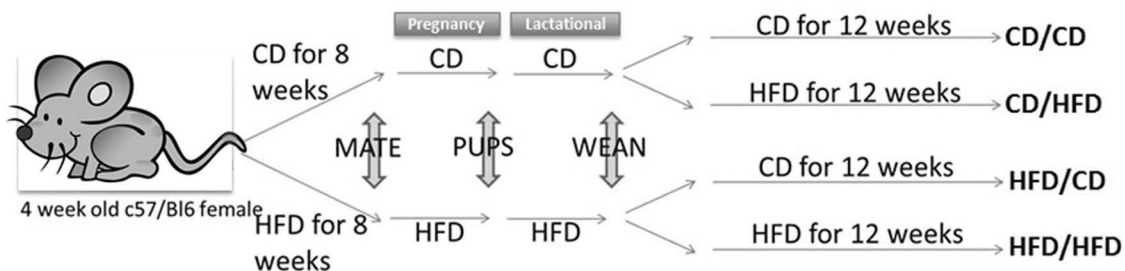


Figure 1. Maternal diet exposure model. Scheme for breeding and experimental diet exposure for each group of offspring. Male and female mice were included in each group.

labeling (TUNEL), or immunohistochemistry (IHC). For IHC, sections were rehydrated by passing through xylene, graded alcohol, and distilled water followed by staining utilizing select primary antibodies (Table 1) and the Vectastain Elite ABC kit (Vector Laboratories, Burlingame, CA, USA) protocol. Antigen retrieval was performed by pressure cooking for 30 min in citrate buffer. After antigen retrieval, endogenous peroxide inactivation, and blocking, sections were incubated with primary antibody for 30 min at room temperature. Sections were then washed and incubated with appropriate biotin-conjugated secondary antibody for 30 min. Sections were washed, incubated with ABC reagent, washed, and incubated with 3,3'-diaminobenzidine. Sections were counterstained with hematoxylin QS solution (Vector) and cover slipped using Cytoseal XYL (Richard Allen Scientific, Kalamazoo, MI, USA).

For evaluation of fibrosis, Sirius red staining was performed by the Morphology Core at The Research Institute at Nationwide Children's Hospital. Proliferation was measured by PCNA staining. TUNEL staining was performed with an in situ apoptosis detection kit (Trevigen, Gaithersburg, MD, USA) according to the manufacturer's protocol. Representative photomicrographs are shown. Morphometric analysis was performed using ImageJ. Positive cell counting was performed with Zeiss ZEN 2011 software. Microscopy and image capture were performed on an Olympus IX51 microscope.

Protein Extraction and Immunoblot Analysis

Tissue lysates were prepared from frozen liver with radio-immunoprecipitation assay buffer (Boston Bioproducts, Ashland, MA, USA) containing HALT protease and phosphatase inhibitor cocktail (Thermo Fisher Scientific, Waltham, MA, USA). Protein concentration was determined using the bicinchoninic acid assay (Pierce, Rockford, IL, USA). Equal amounts of protein from each sample (20–30 µg) were separated on 10% SDS-polyacrylamide gels (Bio-Rad, Hercules, CA, USA) and subsequently transferred to polyvinylidene fluoride or nitrocellulose membranes. Membranes were then blocked in 5% milk and incubated

with anti-osteopontin (R&D Systems, Minneapolis, MN, USA) and anti-GAPDH (loading control; Cell Signaling Technology, Danvers, MA, USA). Species-appropriate horseradish peroxidase-conjugated secondary antibodies (Millipore, Billerica, MA, USA) were used to detect antigen-antibody complexes. Blots were developed using Luminata Classico (Millipore) and exposed to X-ray film. Label-free quantitation was performed using the spectral count approach, in which the relative protein quantitation is measured by comparing the number of tandem mass spectrometry (MS/MS) spectra identified from the same protein in each of the multiple liquid chromatography (LC)/MS/MS data sets. Scaffold was used for quantitation analysis.

Proteome Array and Proteomic Analysis

A proteome array was performed using a Mouse Angiogenesis Array (R&D Systems) following the manufacturer's protocol. Briefly, protein lysates from three livers within each group were pooled and incubated with prehybridized antibody membranes. Total pooled protein was 450 µg for each group. Blots were developed using Luminata Classico reagents and exposed to X-ray film.

Proteomic analysis was performed by the Proteomics and Mass Spectrometry Facility at The Ohio State University on tissue lysates from postnatal day 7 (p7) liver of offspring exposed to maternal HFD or CD. Briefly, samples were prepared by in-gel digestion. The final digests were analyzed using capillary-liquid chromatography-nanospray tandem mass spectrometry (Capillary-LC/MS/MS) of global protein identification and was performed on a Thermo Finnigan LTQ orbitrap mass spectrometer equipped with a microspray source (Michrom Bioresources Inc., Auburn, CA, USA) operated in positive ion mode. Sequence information from the MS/MS data was processed by converting the .raw files into mgf files using MsConvert and later merged into a merged file (.mgf) using an in-house program, RAW2MZXML_n_MGF_batch (merge.pl, a Perl script), and searched using Mascot Daemon by Matrix Science version 2.3.2 (Boston, MA, USA) against the SwissProt mouse database (Version 2015_01, 16,702 sequences).

Table 1. Primary Antibodies for IHC

Antibody	Host	Company	Catalog #	Retrieval	Dilution
α-SMA	Mouse	Dako	M0851	Citrate	1:500
CK19	Rat	Developmental Studies Hybridoma Bank	Troma III	Citrate	1:150
4-Hydroxynonenal	Rabbit	Abcam	Ab46545	Citrate	1:250
PCNA	Mouse	BD Biosciences	610665	Citrate	1:100

The CK19 antibody (Troma III) developed by Dr. Rolf Kemler was obtained from the Developmental Studies Hybridoma Bank, created by the NICHD of the NIH and maintained at The University of Iowa, Department of Biology, Iowa City, IA, USA.

Quantitative RNA Expression Analysis

RNA was isolated from snap-frozen livers of 12-week mice by TRIzol extraction followed by purification using a Qiagen RNeasy Mini Kit and protocol (Qiagen, Valencia, CA, USA). Equivalent amounts of RNA from each sample were reverse transcribed using the Thermo Scientific First Strand cDNA Synthesis Kit (Thermo Fisher Scientific), and the resulting cDNAs were amplified using the Thermo Scientific Maxima Probe/ROX PCR mix (Thermo Fisher Scientific). Primer pairs (Table 2) were designed using the Roche Universal Probe Library Assay Design Center (<https://lifescience.roche.com>) and were used with their corresponding probes during amplification. For relative expression, $\Delta\Delta C_t$ analysis was performed for each target using β -actin (ActB) as the primary normalizer [Ct value (mean \pm standard deviation) = 25.61 \pm 0.41, $n=38$], and the mean value for male CD/CD mice as the secondary normalizer.

Hepatic Triglyceride Assay

Hepatic triglyceride levels in liver tissue homogenates were measured using a Triglyceride Assay Kit (Caymen Chemical, Ann Arbor, MI, USA).

Statistical Analysis

Unpaired Student's *t*-test or two-way repeated-measures analysis of variance (ANOVA) were used when appropriate using GraphPad prism software. Data are presented as mean \pm SD, with $p < 0.05$ representing significance.

RESULTS

Increased Liver and Body Weights in Offspring Exposed to Maternal HFD

Female C57Bl/6J mice were fed HFD or CD for 8 weeks prior to mating (Fig. 1). Livers from the female mice exposed to HFD exhibited no evidence of pathology, comparable to female mice exposed to the CD (Fig. 2A).

Both male and female offspring from dams exposed to HFD exhibited a significant increase in body and liver weights at p7 (Fig. 2B). Histologic evaluation of offspring livers by H&E staining did not show any clear differences over the course from p0 to p21 (Fig. 2C). Liver triglyceride content was not different between maternal HFD- and CD-fed offspring at p0, p7, and p14, but higher liver triglyceride levels were present in maternal HFD-exposed offspring at p21 compared to CD (Fig. 2D).

Stellate Cell Activation in Offspring Exposed to Maternal HFD

To evaluate whether there was evidence of fibrosis in the perinatal period during exposure to maternal HFD, we performed Sirius red staining on livers from pups exposed to maternal CD or HFD. We did not observe any evidence of pericellular fibrosis within the liver parenchyma in either group throughout the perinatal time course (Fig. 2C). IHC for α -smooth muscle actin (α -SMA) was performed to identify activated stellate cells in the liver of offspring. Many activated stellate cells were observed at p0 and p7 in both groups. At subsequent perinatal time points (p14 and p21), liver from mice exposed to CD had no α -SMA-positive stellate cells in the parenchyma, while activated stellate cells were still present in liver from pups exposed to maternal HFD (Fig. 2C).

Increased Hepatocyte and Cholangiocyte Proliferation at Time of Weaning in Offspring Exposed to Maternal HFD

The postnatal liver undergoes a period characterized by significant hepatocyte proliferation. To evaluate whether maternal HFD exposure impacts proliferation and cell turnover, we performed IHC for PCNA and TUNEL on liver from offspring exposed to maternal CD or HFD. A high number of PCNA-positive hepatocytes were present in both groups at p0 and p7, consistent with the expected cell proliferation that occurs during postnatal liver growth

Table 2. Real-Time PCR Primers

Gene	Accession No.	Forward Primer	Reverse Primer
Col1a1	NM_007742	acctaagggtaccgctgga	gagctccagcttctccatctt
Col3a1	NM_009930	tccctggaatctgtgaatc	tgagtcgaattggggagaat
Tgfb1	NM_011577	tcagacattcgggaagcagt	acgccaggaattgttctctat
Tgfb2	NM_009367	aggaggttataaaatcgacatgc	tagaaagtggcggggatg
MMP2	NM_008610	gtgggacaagaaccagatcac	gcatacaccaggtttcag
MMP9	NM_013599	ggatggttaccgctggtg	ctacggtcgcgtccactc
Spp1	NM_009263	ggaggaaccgccaagg	tgccagaatcagtcactttcac
CTGF	NM_010217	ctgcagactggagaagcaga	gatgcactttttgcccttctt
Il1b	NM_008361	agttgacggaccccaaaag	agctggatgctctcatcagg
Il6	NM_031168	gctaccaaactggatataatcagga	ccaggtagctatggatctccagaa
Nfkb1	NM_008689.2	gaccactgctcaggtccact	tgctactatcccgaggttca
Lcn2	NM_008491	ccatctatgagctacaagagaacaat	tctgatccagtagcgacagc
Actb	NM_007393	ctaaggccaaccgtgaaaag	accagaggcatcacagggaca

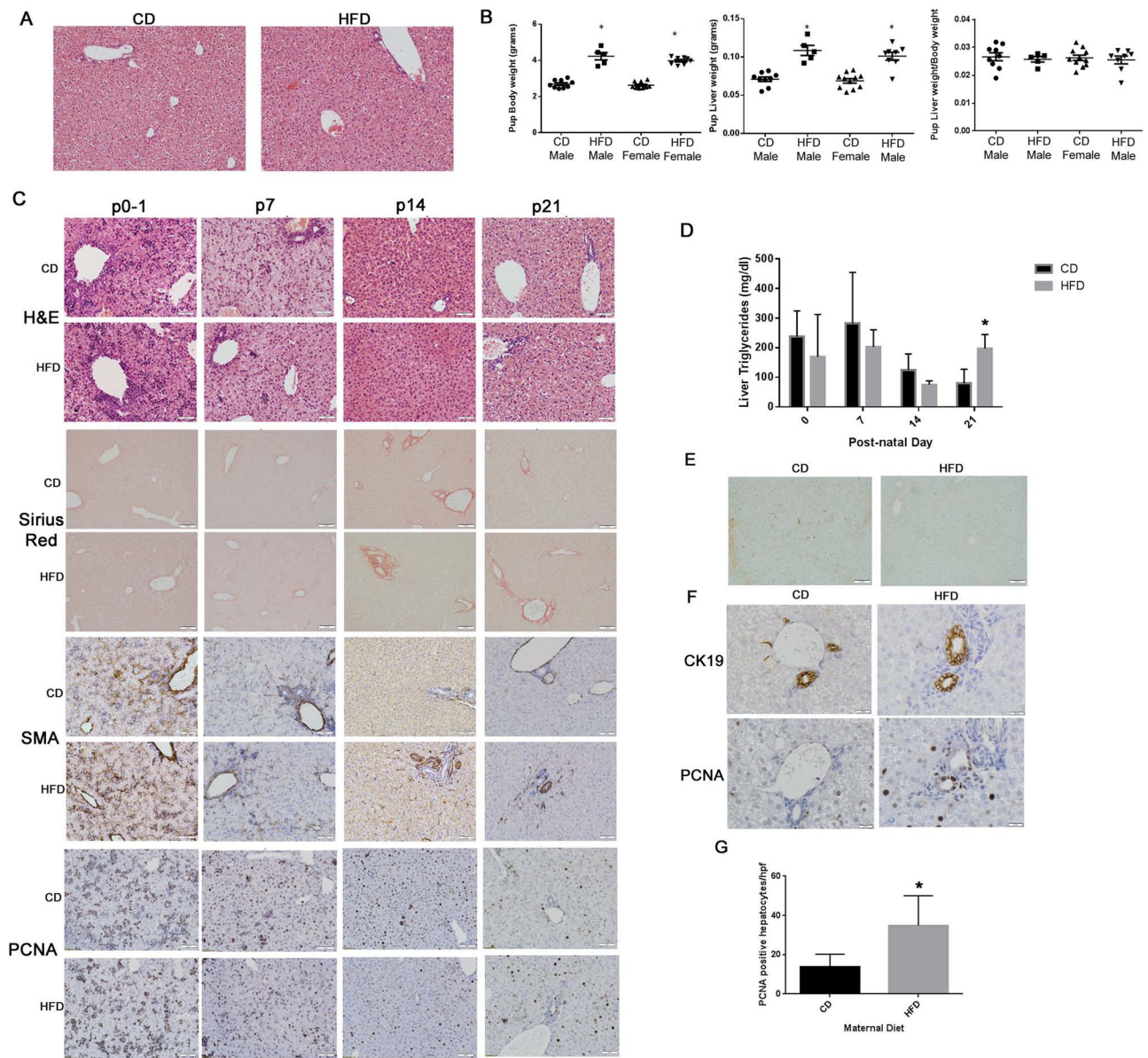


Figure 2. Maternal HFD exposure leads to prolonged stellate cell activation and increased cellular proliferation in perinatal offspring liver. (A) Hematoxylin and eosin (H&E) staining of representative liver from female mice fed HFD for 8 weeks prior to mating. (B) Body weight, liver weight, and body weight/liver weight ratio of maternal CD- or HFD-exposed offspring at p7. (C) Histology and IHC of offspring liver at p0, p7, p14, and p21 exposed to maternal CD or HFD. Representative photomicrographs shown with type of staining labeled on left. Scale bars: 100 μ m (Sirius red), 50 μ m (H&E, α -SMA, and PCNA). (D) Liver triglyceride levels at p0, p7, p14, and p21 from offspring exposed to maternal CD or HFD ($n=3-4$ males per group). (E) TUNEL staining of offspring liver at p21 exposed to maternal CD or HFD. Scale bars: 100 μ m. (F) CK19 and PCNA staining of offspring liver at p21 exposed to maternal CD or HFD, highlighting PCNA-positive cholangiocytes in HFD-exposed offspring. Scale bars: 20 μ m. (G) Quantitation of PCNA-positive hepatocytes in p21 offspring liver exposed to maternal CD or HFD. * $p<0.05$ HFD versus CD.

(Fig. 2C). At p14 and p21, the number of PCNA-positive cells declined in both groups relative to this early postnatal period of postnatal growth. However, the number of positive hepatocytes was significantly higher in the liver of pups exposed to maternal HFD than CD at p21 (Fig. 2G). We also found that there were more PCNA-positive cholangiocytes

[also cytokeratin-19 (CK19) positive] in the liver of p21 pups exposed to maternal HFD compared to maternal CD (Fig. 2F). No clear difference in TUNEL-positive hepatocytes was observed between maternal CD- and HFD-fed pups at p21, suggesting that the increase in proliferation observed is not matched by concomitant cell death at this

time point (Fig. 2E). Interestingly, we identified several TUNEL-positive nonparenchymal cells in the liver of offspring exposed to CD but saw none in the liver of offspring exposed to maternal HFD.

Proteomic Analysis of Liver From Offspring Exposed to Maternal CD or HFD

Protein lysates were made from liver of p7 pups exposed to maternal CD or HFD. The proteins were separated by gel electrophoresis, and proteomic analysis was performed on gel slices. A total of 1,248 proteins were identified in both groups, 75 of which showed a difference in expression between CD and HFD ($p \leq 0.05$). Enrichment analysis was performed on the differentially expressed proteins utilizing the DAVID Bioinformatics Resource and KEGG database. The enriched pathways included PPAR signaling, fatty acid metabolism, citric acid cycle, glycolysis/gluconeogenesis, mitochondria, peroxisomes, and xenobiotic metabolism by cytochrome p450. Specific proteins from the fatty acid metabolism and/or PPAR signaling pathways that were differentially expressed based on spectral counts included fatty acid binding protein, fatty acid desaturase 2, acetyl CoA acetyltransferase, and very long chain acyl-CoA synthetase (Table 3). Several proteins involved in oxidative metabolism were also differentially expressed including fumarate hydratase, peroxiredoxin-6, catalase, and thioredoxin-like protein 1.

Progressive Pathology in Adult Offspring Previously Exposed to Maternal HFD Including Severe Steatosis and Fibrosis

To evaluate the long-term impact of maternal HFD exposure on the offspring liver, maternal CD- and

HFD-exposed pups were weaned at 20 days old and placed on either CD or HFD for 12 weeks. This created four groups for analysis: maternal CD-offspring CD (CD/CD), maternal CD-offspring HFD (CD/HFD), maternal HFD-offspring CD (HFD/CD), and maternal HFD-offspring HFD (HFD/HFD). Male and female offspring were included in each group. Both male and female offspring in all four groups gained weight during the study, with more weight gain observed in the male CD/HFD and HFD/HFD groups (Fig. 3A). Male HFD/HFD mice achieved a significantly higher final body weight than male CD/HFD mice ($p < 0.05$). No significant increase in liver weight was observed in either male or female mice exposed to offspring HFD (CD/HFD, HFD/HFD) compared to CD/CD mice (Fig. 3B). However, the liver weight of male HFD/CD was significantly decreased compared to male CD/CD. No differences in fasting glucose levels were observed between male CD/CD and CD/HFD mice (Fig. 3C). Male HFD/CD mice had fasting glucose measurements that were significantly lower than CD/CD and CD/HFD mice throughout the time course ($p \leq 0.01$ at all time points comparing male HFD/CD to CD/CD or CD/HFD). HFD/HFD male mice had lower fasting glucose levels than CD/CD and CD/HFD mice at 1 week, but this difference was lost by 5 weeks. No significant differences in fasting glucose levels were observed between any of the groups of female mice. Food intake was similar between all groups (Fig. 3D).

H&E staining revealed that male CD/HFD mice exhibited hepatic steatosis after 12 weeks of HFD feeding and that male HFD/HFD mice showed a more severe steatotic response (Fig. 3E), as previously reported¹⁰. Interestingly, male HFD/CD mice showed both micro- and

Table 3. Fold Change of Selected Proteins

Protein	Fold Change (HFD/CD)	<i>p</i> Value
Fatty acid-binding protein	1.41	0.0017
Fumarate hydratase, mitochondrial	1.20	0.0035
Cytochrome P450 2E1	0.71	0.0085
Peroxisomal acyl-coenzyme A oxidase 1	0.61	0.012
Pyruvate dehydrogenase E1 component subunit alpha, somatic form, mitochondrial	0.60	0.012
Adenylyl cyclase-associated protein 1	0.71	0.021
Peroxiredoxin-6	1.26	0.024
Very long chain acyl-CoA synthetase	0.77	0.027
Catalase	0.88	0.03
Fatty acid desaturase 2	0.56	0.031
Quinone oxidoreductase	0.55	0.037
Thioredoxin-like protein 1	0.82	0.039
Fibronectin	1.59	0.042
Acetyl-CoA acetyltransferase, mitochondrial	0.85	0.046

Fold change of spectral counts ($n=3$ male liver homogenates) of selected proteins identified to be significantly over- or underexpressed in p7 offspring liver exposed to maternal HFD compared to CD.

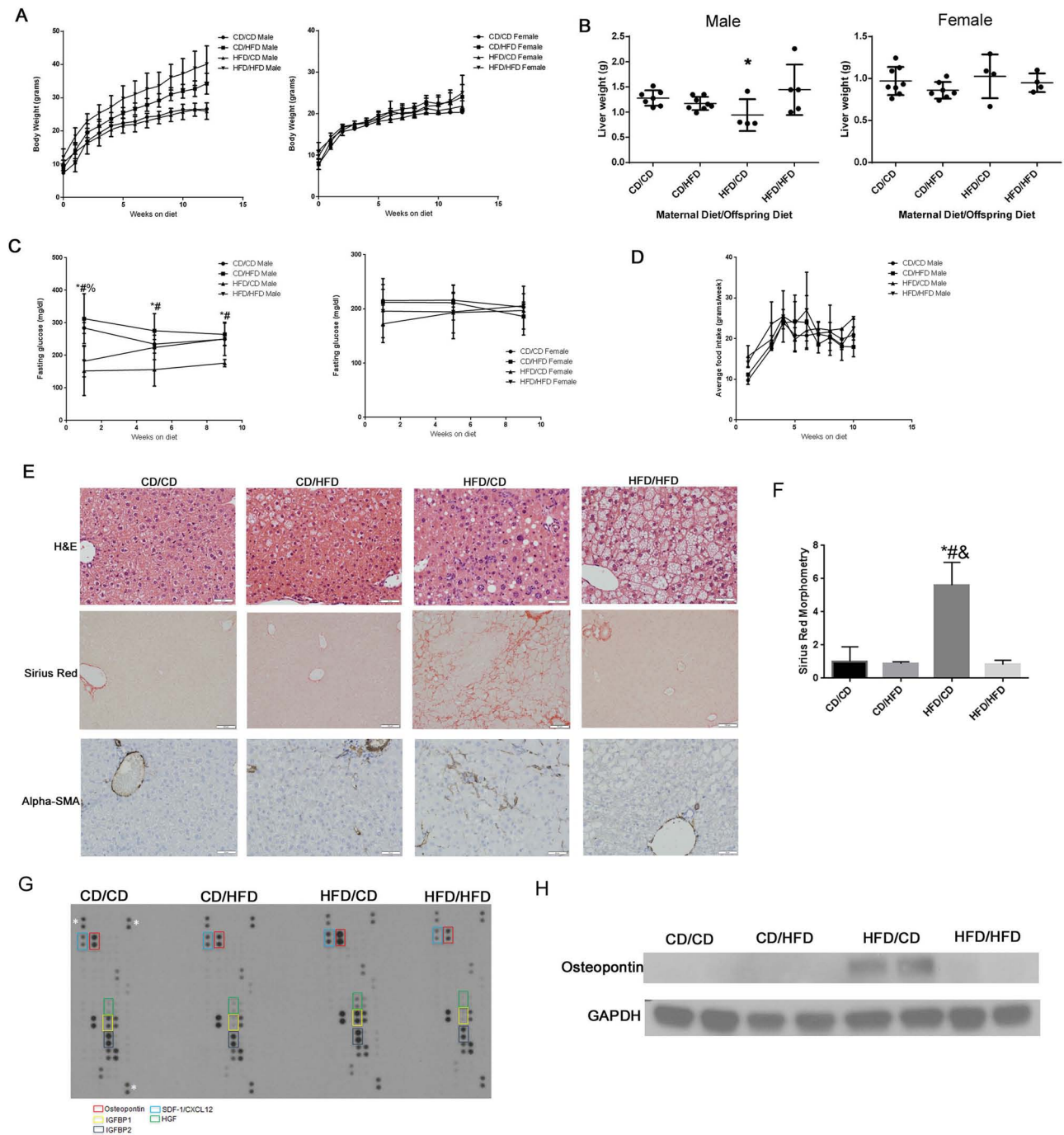


Figure 3. Progressive pathology in adult offspring previously exposed to maternal HFD. (A) Body weight of male and female mice over the time course of postweaning diet exposure ($n=4-9$ per group). (B) Final liver weights of male and female mice after perinatal CD or HFD exposure followed by 12 weeks of postweaning CD or HFD. (C) Fasting glucose levels of mice at three time points during the course of postweaning diet exposure. (D) Average food intake (grams/week) over the course of the study. (E) Histology and IHC of adult offspring liver following perinatal CD or HFD exposure and 12 weeks of postweaning CD or HFD. Top row: H&E staining. Scale bars: 50 μm . Middle row: Sirius red staining. Scale bars: 100 μm . Bottom row: IHC for α -SMA. Scale bars: 50 μm . (F) Morphometric analysis of Sirius red staining ($n=5$ livers per group with three fields/liver analyzed). (G) Photomicrograph of proteome array performed on pooled protein lysates ($n=3$) from liver of offspring from each group. White asterisks denote loading control dots. Colored boxes identify select proteins on the array. (H) Representative photomicrograph of Western blot for osteopontin in adult offspring liver from each group. GAPDH is shown as a loading control. * $p<0.05$ HFD/CD versus CD/CD, # $p<0.05$ HFD/CD versus CD/HFD, & $p<0.05$ HFD/CD versus HFD/HFD, % $p<0.05$ HFD/HFD versus CD/CD.

macrovesicular steatosis with associated inflammatory infiltrate. We performed Sirius red staining to evaluate fibrosis in each group. No Sirius red staining beyond the portal and perivascular areas in livers of male CD/CD or CD/HFD mice was observed, and only minimal Sirius red staining was observed in the liver parenchyma of male HFD/HFD mice. In contrast, HFD/CD mice developed pericellular fibrosis throughout the liver (Fig. 3E). Morphometric analysis confirmed the increase in Sirius red staining in the HFD/CD group (Fig. 3F). This phenotype was observed in five of seven male HFD/CD mice but in only three of seven female HFD/CD mice, suggesting phenotypic variation and/or increased sensitivity in the male offspring. IHC for α -SMA showed the presence of many activated stellate cells in both male and female HFD/CD mice consistent with a profibrotic response in the liver (Fig. 3E). By contrast, only a few activated stellate cells were present in the liver of HFD/HFD mice. Proteome array analysis of fibrosis-related factors revealed that expression of osteopontin, IGFBP1, IGFBP2, SDF-1, and hepatocyte growth factor was increased in male HFD/CD mouse livers (Fig. 3G). An increase in expression in the HFD/CD group of osteopontin (reported to be upregulated in other fibrosis models¹⁵⁻¹⁷) was independently confirmed by immunoblot analysis and RT-PCR (Figs. 3H and 4A). Gene expression of several factors involved in fibrosis was measured by RT-PCR (Fig. 4A). Levels of collagen type 1 α 1, collagen type 3 α 1, transforming growth factor- β 1, transforming growth factor- β 2, and matrix metalloproteinase-2 were all significantly increased in male HFD/CD liver compared to all other groups. Interestingly, no significant differences were observed in females, likely accounting for the decreased frequency of fibrosis development in females. Connective tissue growth factor (CTGF) expression trended toward an increase in male HFD/CD compared to male CD/CD ($p=0.15$), but levels in both groups exposed to postweaning HFD had decreased levels compared to male CD/CD and HFD/CD mice.

Gene expression of two proinflammatory cytokines, interleukin-1 β (IL-1 β) and IL-6, was measured in each group (Fig. 4B). There was a significant decrease in levels of IL-1 β male HFD/HFD liver compared to male CD/CD liver with a trend toward a decrease in CD/HFD and HFD/CD. There was also a significant decrease in IL-6 expression levels in male mice exposed to postweaning HFD. No differences in IL-6 expression levels were observed in the female offspring. Overall, the cytokine expression levels do not support an increase in inflammation after maternal or postweaning HFD exposure. However, there was a significant increase in expression of nuclear factor- κ B in male HFD/CD liver compared to all other groups (Fig. 4C).

Increased Proliferation, Apoptosis, Ductular Reaction, and Oxidative Stress in Liver of HFD/CD Offspring

Given the presence of differing pathology in the HFD/CD and HFD/HFD groups at 12 weeks postweaning, we next assessed cellular turnover by measuring proliferation and apoptosis in the liver. PCNA staining showed minimal hepatocyte proliferation in the CD/CD [4 cells/high-power field (hpf)], CD/HFD (4 cells/hpf), and HFD/HFD (3.9 cells/hpf) groups, whereas diffuse hepatocyte proliferation was observed in HFD/CD (21.3 cells/hpf) liver with significantly more PCNA-positive cells (Fig. 5A and B). There was also increased apoptosis in HFD/CD liver shown by TUNEL staining (Fig. 5A and C). This supports an overall increase in cell turnover for offspring exposed to maternal HFD and placed on a CD at weaning.

To evaluate for ongoing oxidative stress in the adult offspring, we performed IHC for 4-hydroxynonenal (4-HNE), a commonly used marker of oxidative stress in the setting of lipotoxicity. No staining for 4-HNE was observed in CD/CD or CD/HFD liver (Fig. 5A and C). However, some staining was observed in HFD/HFD liver, and robust staining for 4-HNE was evident in HFD/CD liver. This suggests increased oxidative stress in both groups previously exposed to maternal HFD with a more dramatic increase in the HFD/CD liver. There was also a significant increase in lipocalin-2 expression, known to be increased in oxidative stress¹⁸, in male HFD/CD offspring liver (Fig. 4D).

A ductular reaction, characterized by the presence of CK19-positive cells emanating into the parenchyma, has been frequently described in the setting of liver injury, is associated with fibrosis¹⁹⁻²¹, and has been observed in mice placed on a methionine- and choline-deficient diet to induce NASH²². We performed CK19 IHC, which showed the presence of many CK19-positive cells emanating into the parenchyma of HFD/CD liver (Fig. 5A and D). This provides evidence of a ductular reaction occurring in HFD/CD liver along with the presence of fibrosis.

DISCUSSION

In agreement with previous studies^{10,23}, we found that the rate of development and degree of steatosis were greater in mice exposed to maternal HFD compared to maternal CD. Previous reports have noted that expression of α -SMA and collagen type 1 α 1 are increased with maternal HFD, but development of fibrosis was not evaluated²⁴. The purpose of the current study was to evaluate whether maternal HFD exposure would lead to enhanced fibrosis and stellate cell activation especially upon reexposure of the offspring to HFD. Minimal fibrosis and stellate cell activation occurred in the offspring of dams fed a HFD and placed on HFD postweaning. We unexpectedly

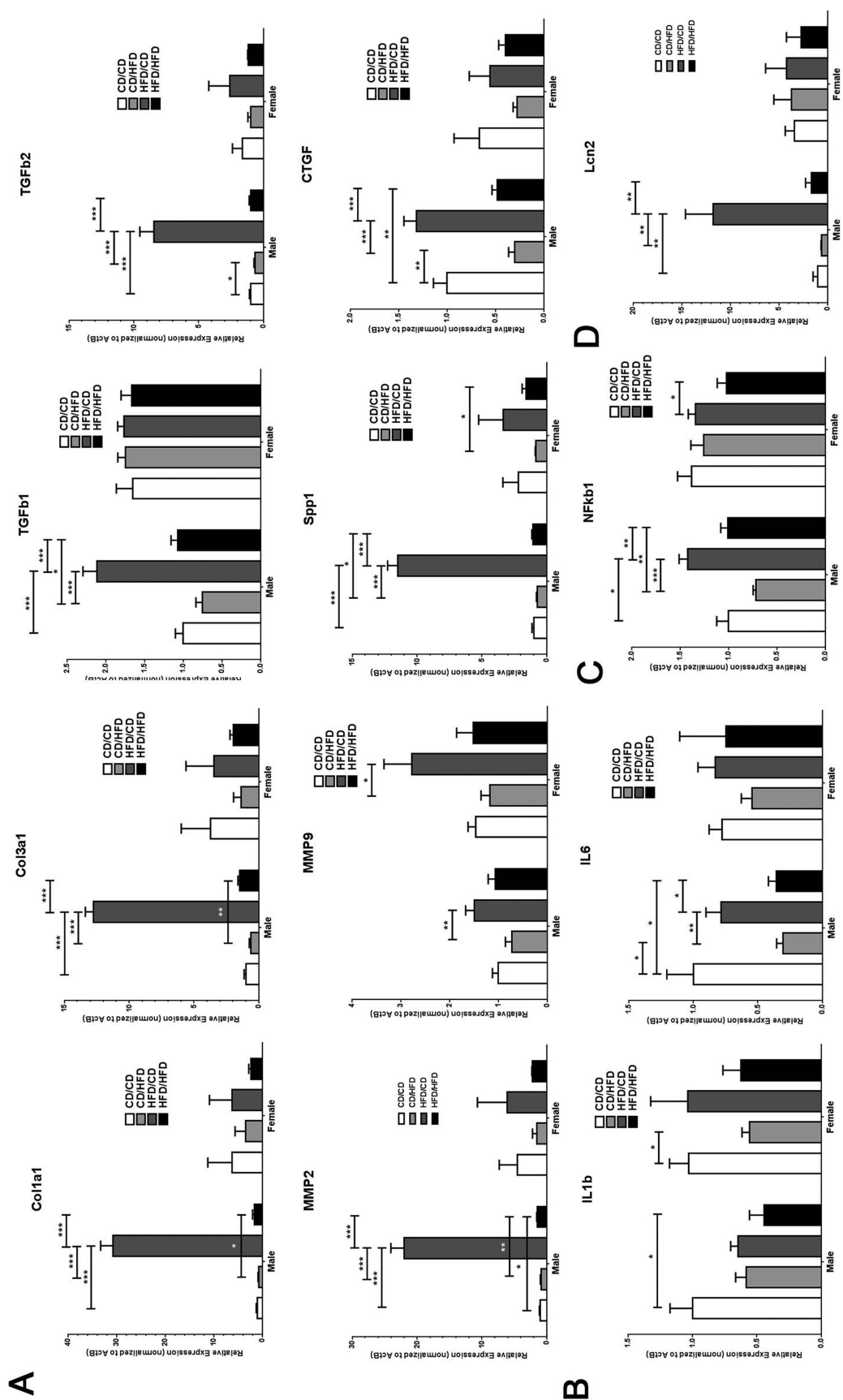
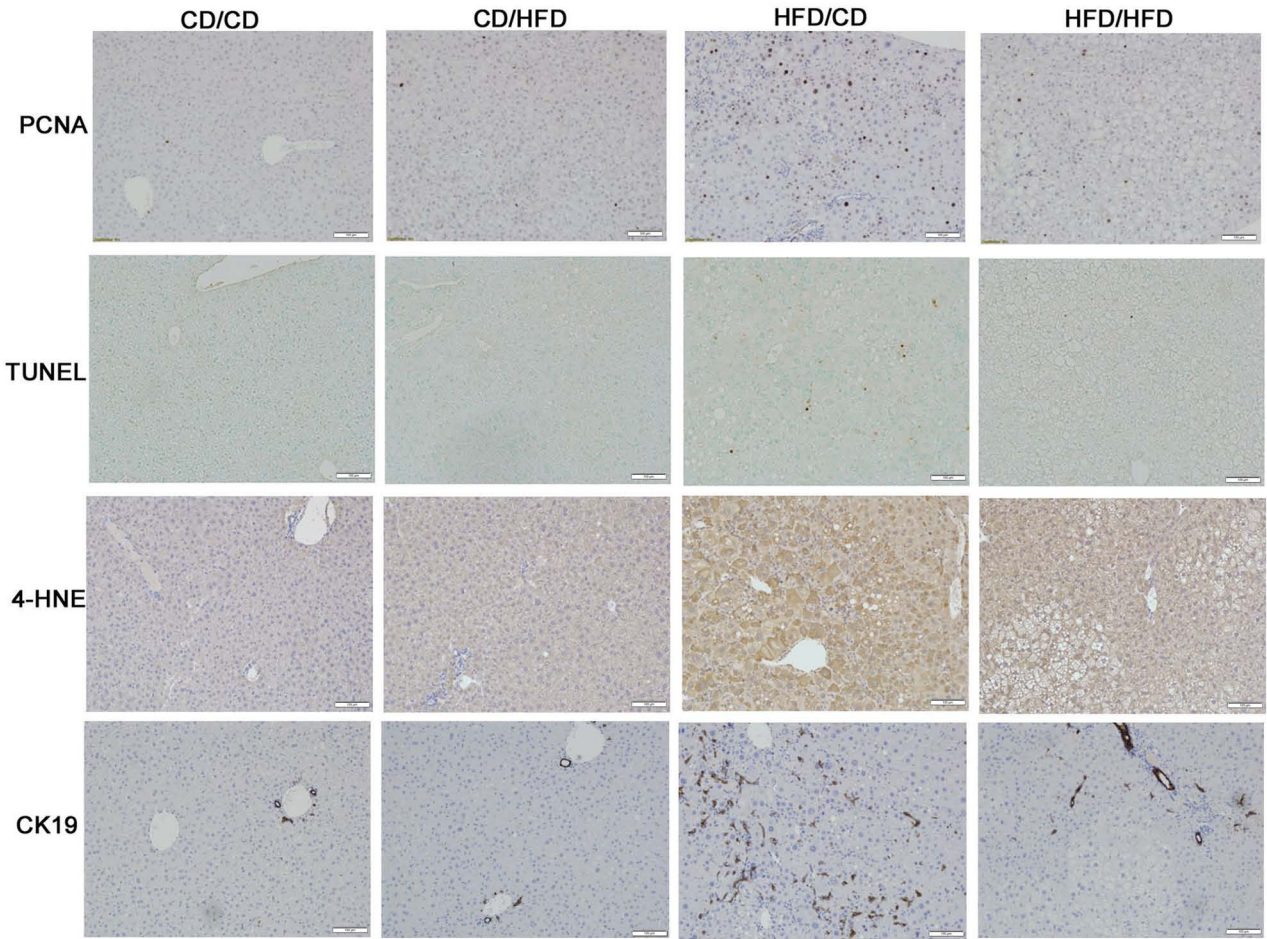
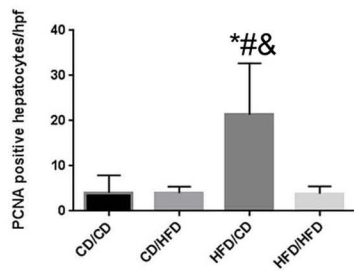


Figure 4. Gene expression of markers of fibrosis, inflammation, and oxidative stress in adult offspring. (A) RT-PCR data for various factors involved in fibrosis. (B) RT-PCR data for proinflammatory cytokines. (C) RT-PCR data for NF- κ B. (D) RT-PCR data for lipocalin-2. All data are presented as relative expression normalized to actin expression with secondary normalization to the average for CD/CD male. * $p < 0.05$, ** $p < 0.01$, *** $p < 0.001$, **** $p < 0.0001$. Col1a1, collagen type 1 alpha 1; Col3a1, collagen type 3 alpha 1; TGF- β , transforming growth factor- β ; MMP, matrix metalloproteinase; Spp1, osteopontin; CTGF, connective tissue growth factor; IL, interleukin; Nfkb1, nuclear factor kappa B; Lcn2, lipocalin-2.

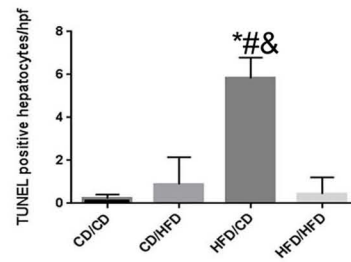
A



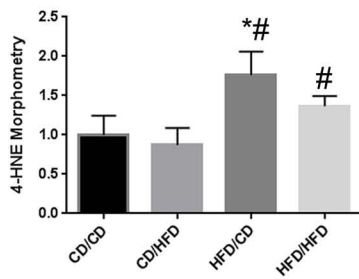
B



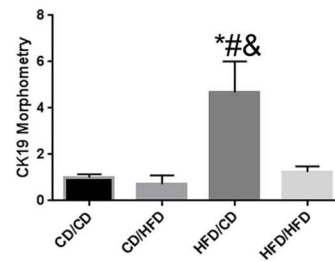
C



D



E



found that the HFD/CD offspring exhibited micro- and macrovesicular steatosis and abundant pericellular fibrosis with associated stellate cell activation. The hepatic histology in HFD/CD offspring was more severe than that previously reported^{9,10} and may be due, in part, to our use of a diet with a higher fat content (60% kcal from fat vs. \leq 45% kcal from fat).

It is counterintuitive that the HFD/CD group developed fibrosis while the HFD/HFD group did not. One possible explanation is that postweaning exposure to HFD actually confers protection from the maternal traits that otherwise render the offspring more fibrosis susceptible. Alternatively, others have reported that in mice, HFD leads to steatosis only and that it takes additional insults, such as fructose or cholesterol, to promote fibrosis²⁵. The cause for this observation has yet to be identified, but one possibility relates to PPAR γ signaling. PPAR γ is increased in the liver during HFD exposure and plays a major role in lipid metabolism. However, PPAR γ blocks the activation of HSCs^{26,27}. Unabated PPAR γ signaling during HFD exposure may block stellate cell activation in this model. We also present here that levels of CTGF gene expression decrease when mice are placed on postweaning HFD. Further analysis will be necessary to delineate the mechanisms of protection from fibrosis observed with postweaning HFD exposure.

Our finding that fibrosis developed in HFD/CD offspring indicates that perinatal exposure to poor maternal nutrition and obesity is sufficient to induce long-term development of liver fibrosis. Although prevalence of fibrosis was not reported, \sim 33% of patients with steatosis on ultrasound are not obese, supporting the notion that factors other than directly consumed diet may lead to NAFLD²⁸. Also, it is widely reported that dietary changes may not be successful in disease resolution in some patients with NAFLD²⁹. It is possible that some patients may not respond to dietary modification due to persistent molecular changes that are a result of perinatal exposure to poor nutrition. If this is true, then alternative strategies in addition to lifestyle modification will need to be developed for this population.

A recent study identified that the presence of fibrosis is the strongest predictor of outcome in patients with NAFLD¹⁴. Retrospective analysis of 691 patients with NAFLD showed that the fibrosis stage was a predictor of

need for liver transplantation and that patients with fibrosis, regardless of steatohepatitis or NAFLD activity score, had shorter survival times than patients without fibrosis. Understanding fibrogenesis in NAFLD is of particular relevance to children with obesity because a unique feature of pediatric NAFLD is the tendency for children to develop steatosis and inflammation in the periportal region rather than the pericentral distribution observed in adult NAFLD³⁰; 51% of children with NAFLD had type 2 NASH characterized by steatosis, portal inflammation, and portal fibrosis. It is also clear that periportal disease distribution is associated with an increase in fibrosis and more advanced liver disease³¹. In our model, HFD/CD liver had fairly diffuse pericellular fibrosis, so it is not clear whether this pathology starts periportal. Regardless of the region of disease, developing a better understanding of why and how some patients are more prone to develop fibrosis will lay the groundwork for creation of novel effective therapies to prevent disease progression. Identification of maternal obesity as a risk factor will also provide insight into those patients who would benefit the most from treatment.

While the mechanism for more severe disease in offspring exposed to perinatal HFD is unclear, several groups have shown pervasive expression changes in genes involved in oxidative stress, metabolism, and inflammation as late as 30 weeks of age following perinatal HFD exposure regardless of the postweaning diet^{10,23,32}. Such permanent alterations in gene expression could be due to genetic imprinting via DNA methylation or acetylation, chromatin remodeling, or possibly microRNA regulation. While such a mechanism has yet to be elucidated, Cannon et al. showed that even though pervasive gene expression changes occur in this model, no change in global DNA methylation was observed³³. Alternatively, HFD exposure in utero and/or postnatally may impact the maternal passage of mitochondria, which could weaken the cell's ability to respond to oxidative stress. Indeed, exposure to maternal HFD results in decreased hepatic mitochondrial DNA content in the offspring¹¹. Since HFD/CD adult offspring exhibit persistent HSC activation and significant pericellular fibrosis that is associated with oxidative stress, hepatocyte turnover, and ductular reaction, future studies focusing on the mechanism behind this increased susceptibility to metabolic derangement, inflammation, and fibrosis will be essential.

FACING PAGE

Figure 5. Increased hepatocyte turnover and ductular reaction in liver of HFD/CD offspring. (A) Staining and IHC of adult offspring liver following perinatal CD or HFD exposure and 12 weeks of postweaning CD or HFD. Representative photomicrographs shown with type of staining labeled on the left. Scale bars: 100 μ m for all images. (B) Quantitation of PCNA-positive hepatocytes from each group ($n=4-5$ livers per group with three fields/liver counted). (C) Quantitation of TUNEL-positive hepatocytes from each group ($n=3-4$ livers per group with three fields/liver counted). (D) Morphometric analysis of 4-HNE staining ($n=3$ livers per group with three fields/liver analyzed). (E) Morphometric analysis of CK19 staining ($n=3$ livers per group with three fields/liver analyzed). * $p<0.05$ versus CD/CD, # $p<0.05$ versus CD/HFD, & $p<0.05$ versus HFD/HFD.

An intriguing and unanticipated finding in this study was increased hepatocyte proliferation in HFD/CD offspring. This may be the result of activation of repair mechanisms to balance ongoing injury in these mice. Zhang et al. showed altered expression of several microRNAs that may impact cell cycle control following exposure to maternal HFD³². For example, miR-16, a negative regulator of cyclin D1, was decreased after perinatal HFD exposure³⁴. Converse to this and our findings, expression of the cell cycle inhibitor, Cdkn1a, was increased in rat offspring liver after maternal HFD exposure due to hypomethylation of the Cdkn 1a promoter³⁵. We also observed an increased ductular reaction in liver of offspring exposed to maternal HFD as evidenced by parenchymal infiltration of CK19-positive cells. This ductular reaction is believed to be composed of progenitor cells with the capability of producing new hepatocytes and cholangiocytes in the setting of injury^{36,37}. A link has previously been noted between the appearance of this ductular reaction and the development of hepatic fibrosis²⁰. Hepatic progenitor cells are present in pediatric NAFLD and independently associated with the degree of fibrosis¹⁹, but their mechanistic role in hepatic pathology has yet to be determined.

In summary, an important and novel finding in this study was that exposure to maternal HFD leads to HSC activation and development of fibrosis in the liver of some adult offspring. The implication that such an early life exposure has long-term consequences on liver pathology in the offspring is relevant to better understand disease progression in NAFLD. Future studies will need to focus on the molecular mechanisms involved in the cellular and gross pathology noted in our model to evaluate whether preventative therapies can be targeted to prevent progression of NAFLD. It is also reasonable to anticipate that if maternal HFD exposure leads to increased sensitivity to fibrosis development in NAFLD, the same may be true for the development of fibrosis in many other chronic liver diseases. Utilizing models of maternal HFD exposure will delineate the global impact of such risk and provide a way to identify and target those patients that will eventually develop liver fibrosis.

ACKNOWLEDGMENTS: This study was funded by The Research Institute at Nationwide Children's Hospital. M.D.T. is supported by the Sotos/Wolfe Fellowship in Endocrinology. The authors declare no conflicts of interest.

REFERENCES

- Giorgio V, Prono F, Graziano F, Nobili V. Pediatric non alcoholic fatty liver disease: Old and new concepts on development, progression, metabolic insight and potential treatment targets. *BMC Pediatr.* 2013;13:40.
- Bellentani S, Scaglioni F, Marino M, Bedogni G. Epidemiology of non-alcoholic fatty liver disease. *Dig Dis.* 2010;28(1):155–61.
- Barker DJ, Bull AR, Osmond C, Simmonds SJ. Fetal and placental size and risk of hypertension in adult life. *BMJ* 1990;301(6746):259–62.
- Barker DJ, Gluckman PD, Godfrey KM, Harding JE, Owens JA, Robinson JS. Fetal nutrition and cardiovascular disease in adult life. *Lancet* 1993;341(8850):938–41.
- Hanson MA, Gluckman PD. Early developmental conditioning of later health and disease: Physiology or pathophysiology? *Physiol Rev.* 2014;94(4):1027–76.
- Hinkle SN, Sharma AJ, Kim SY, Park S, Dalenius K, Brindley PL, Grummer-Strawn LM. Prepregnancy obesity trends among low-income women, United States, 1999–2008. *Matern Child Health J.* 2012;16(7):1339–48.
- Stamnes Kopp UM, Dahl-Jorgensen K, Stigum H, Frost Andersen L, Naess O, Nystad W. The associations between maternal pre-pregnancy body mass index or gestational weight change during pregnancy and body mass index of the child at 3 years of age. *Int J Obes. (Lond.)* 2012;36(10):1325–31.
- Whitaker RC. Predicting preschooler obesity at birth: The role of maternal obesity in early pregnancy. *Pediatrics* 2004;114(1):e29–36.
- Mouralidarane A, Soeda J, Visconti-Pugmire C, Samuelsson AM, Pombo J, Maragkoudaki X, Butt A, Saraswati R, Novelli M, Fusai G and others. Maternal obesity programs offspring nonalcoholic fatty liver disease by innate immune dysfunction in mice. *Hepatology* 2013;58(1):128–38.
- Bruce KD, Cagampang FR, Argenton M, Zhang J, Ethirajan PL, Burdge GC, Bateman AC, Clough GF, Poston L, Hanson MA and others. Maternal high-fat feeding primes steatohepatitis in adult mice offspring, involving mitochondrial dysfunction and altered lipogenesis gene expression. *Hepatology* 2009;50(6):1796–808.
- Burgueno AL, Cabrerizo R, Gonzales Mansilla N, Sookoian S, Pirola CJ. Maternal high-fat intake during pregnancy programs metabolic-syndrome-related phenotypes through liver mitochondrial DNA copy number and transcriptional activity of liver PPARGC1A. *J Nutr Biochem.* 2013;24(1):6–13.
- Thorn SR, Baquero KC, Newsom SA, El Kasmi KC, Bergman BC, Shulman GI, Grove KL, Friedman JE. Early life exposure to maternal insulin resistance has persistent effects on hepatic NAFLD in juvenile nonhuman primates. *Diabetes* 2014;63(8):2702–13.
- Brumbaugh DE, Friedman JE. Developmental origins of nonalcoholic fatty liver disease. *Pediatr Res.* 2014;75(1–2):140–7.
- Angulo P, Kleiner DE, Dam-Larsen S, Adams LA, Bjornsson ES, Charatcharoenwitthaya P, Mills PR, Keach JC, Lafferty HD, Stahler A, Haflidadottir S, Bendtsen F. Liver fibrosis, but no other histologic features, is associated with long-term outcomes of patients with nonalcoholic fatty liver disease. *Gastroenterology* 2015;149(2):389–97 e10.
- Coombes JD, Choi SS, Swiderska-Syn M, Manka P, Reid DT, Palma E, Briones-Orta MA, Xie G, Younis R, Kitamura N, Della Peruta M, Bitencourt S, Dollé L, Oo YH, Mi Z, Kuo PC, Williams R, Chokshi S, Canbay A, Claridge LC, Eksteen B, Diehl AM, Syn WK. Osteopontin is a proximal effector of leptin-mediated non-alcoholic steatohepatitis (NASH) fibrosis. *Biochim Biophys Acta* 2016; 1862(1):135–44.
- Syn WK, Choi SS, Liaskou E, Karaca GF, Agboola KM, Oo YH, Mi Z, Pereira TA, Zdanowicz M, Malladi P,

- Chen Y, Moylan C, Jung Y, Bhattacharya SD, Teaberry V, Omenetti A, Abdelmalek MF, Guy CD, Adams DH, Kuo PC, Michelotti GA, Whittington PF, Diehl AM. Osteopontin is induced by hedgehog pathway activation and promotes fibrosis progression in nonalcoholic steatohepatitis. *Hepatology* 2011;53(1):106–15.
17. Fickert P, Thueringer A, Moustafa T, Silbert D, Gumhold J, Tsybrovskyy O, Lebofsky M, Jaeschke H, Denk H, Trauner M. The role of osteopontin and tumor necrosis factor alpha receptor-1 in xenobiotic-induced cholangitis and biliary fibrosis in mice. *Lab Invest.* 2010;90(6):844–52.
 18. Roudkenar MH, Kuwahara Y, Baba T, Roushanded AM, Ebishima S, Abe S, Ohkubo Y, Fukumoto M. Oxidative stress induced lipocalin 2 gene expression: Addressing its expression under the harmful conditions. *J Radiat Res.* 2007;48(1):39–44.
 19. Nobili V, Carpino G, Alisi A, Franchitto A, Alpini G, De Vito R, Onori P, Alvaro D, Gaudio E. Hepatic progenitor cells activation, fibrosis, and adipokines production in pediatric nonalcoholic fatty liver disease. *Hepatology* 2012;56(6):2142–53.
 20. Williams MJ, Clouston AD, Forbes SJ. Links between hepatic fibrosis, ductular reaction, and progenitor cell expansion. *Gastroenterology* 2014;146(2):349–56.
 21. Machado MV, Michelotti GA, Pereira TA, Xie G, Premont R, Cortez-Pinto H, Diehl AM. Accumulation of duct cells with activated YAP parallels fibrosis progression in non-alcoholic fatty liver disease. *J Hepatol.* 2015;63(4):962–70.
 22. Machado MV, Michelotti GA, Xie G, Almeida Pereira T, Boursier J, Bohnic B, Guy CD, Diehl AM. Mouse models of diet-induced nonalcoholic steatohepatitis reproduce the heterogeneity of the human disease. *PLoS One* 2015;10(5):e0127991.
 23. Alfaradhi MZ, Fernandez-Twinn DS, Martin-Gronert MS, Musial B, Fowden A, Ozanne SE. Oxidative stress and altered lipid homeostasis in the programming of offspring fatty liver by maternal obesity. *Am J Physiol Regul Integr Comp Physiol.* 2014;307(1):R26–34.
 24. Oben JA, Mouralidarane A, Samuelsson AM, Matthews PJ, Morgan ML, McKee C, Soeda J, Fernandez-Twinn DS, Martin-Gronert MS, Ozanne SE, et al. Maternal obesity during pregnancy and lactation programs the development of offspring non-alcoholic fatty liver disease in mice. *J Hepatol.* 2010;52(6):913–20.
 25. Sanches SC, Ramalho LN, Augusto MJ, da Silva DM, Ramalho FS. Nonalcoholic steatohepatitis: A search for factual animal models. *Biomed Res Int.* 2015;2015:574832.
 26. Marra F, Efsen E, Romanelli RG, Caligiuri A, Pastacaldi S, Batignani G, Bonacchi A, Caporale R, Laffi G, Pinzani M, Gentilini P. Ligands of peroxisome proliferator-activated receptor gamma modulate profibrogenic and proinflammatory actions in hepatic stellate cells. *Gastroenterology* 2000;119(2):466–78.
 27. Galli A, Crabb D, Price D, Ceni E, Salzano R, Surrenti C, Casini A. Peroxisome proliferator-activated receptor gamma transcriptional regulation is involved in platelet-derived growth factor-induced proliferation of human hepatic stellate cells. *Hepatology* 2000;31(1):101–8.
 28. Williams CD, Stengel J, Asike MI, Torres DM, Shaw J, Contreras M, Landt CL, Harrison SA. Prevalence of nonalcoholic fatty liver disease and nonalcoholic steatohepatitis among a largely middle-aged population utilizing ultrasound and liver biopsy: A prospective study. *Gastroenterology* 2011;140(1):124–31.
 29. Wang RT, Koretz RL, Yee HF Jr. Is weight reduction an effective therapy for nonalcoholic fatty liver? A systematic review. *Am J Med.* 2003;115(7):554–9.
 30. Schwimmer JB, Behling C, Newbury R, Deutsch R, Nievergelt C, Schork NJ, Lavine JE. Histopathology of pediatric nonalcoholic fatty liver disease. *Hepatology* 2005;42(3):641–9.
 31. Brunt EM, Kleiner DE, Wilson LA, Unalp A, Behling CE, Lavine JE, Neuschwander-Tetri BA, Appendix NCRNlomotNSCRNcbfit. Portal chronic inflammation in nonalcoholic fatty liver disease (NAFLD): A histologic marker of advanced NAFLD-clinicopathologic correlations from the nonalcoholic steatohepatitis clinical research network. *Hepatology* 2009;49(3):809–20.
 32. Zhang J, Zhang F, Didelot X, Bruce KD, Cagampang FR, Vatish M, Hanson M, Lehnert H, Ceriello A, Byrne CD. Maternal high fat diet during pregnancy and lactation alters hepatic expression of insulin like growth factor-2 and key microRNAs in the adult offspring. *BMC Genomics* 2009;10:478.
 33. Cannon MV, Buchner DA, Hester J, Miller H, Sehayek E, Nadeau JH, Serre D. Maternal nutrition induces pervasive gene expression changes but no detectable DNA methylation differences in the liver of adult offspring. *PLoS One* 2014;9(3):e90335.
 34. Bonci D, Coppola V, Musumeci M, Addario A, Giuffrida R, Memeo L, D'Urso L, Pagliuca A, Biffoni M, Labbaye C and others. The miR-15a-miR-16-1 cluster controls prostate cancer by targeting multiple oncogenic activities. *Nat Med.* 2008;14(11):1271–7.
 35. Dudley KJ, Sloboda DM, Connor KL, Beltrand J, Vickers MH. Offspring of mothers fed a high fat diet display hepatic cell cycle inhibition and associated changes in gene expression and DNA methylation. *PLoS One* 2011;6(7):e21662.
 36. Roskams TA, Theise ND, Balabaud C, Bhagat G, Bhathal PS, Bioulac-Sage P, Brunt EM, Crawford JM, Crosby HA, Desmet V, Finegold MJ, Geller SA, Gouw AS, Hytiroglou P, Knisely AS, Kojiro M, Lefkowitz JH, Nakanuma Y, Olynyk JK, Park YN, Portmann B, Saxena R, Scheuer PJ, Strain AJ, Thung SN, Wanless IR, West AB. Nomenclature of the finer branches of the biliary tree: Canals, ductules, and ductular reactions in human livers. *Hepatology* 2004;39(6):1739–45.
 37. Dorrell C, Erker L, Schug J, Kopp JL, Canaday PS, Fox AJ, Smirnova O, Duncan AW, Finegold MJ, Sander M, et al. Prospective isolation of a bipotential clonogenic liver progenitor cell in adult mice. *Genes Dev.* 2011;25(11):1193–203.